Xu et al. Journal of Ovarian Research (2025) 18:49
https://doi.org/10.1186/s13048-025-01627-0

Journal of Ovarian Research

RESEARCH Open Access

Intrinsic differences in mTOR activity mediates lineage-specific responses to cyclophosphamide in mouse and human granulosa cells

Shiqian Xu[1,2,4,5], Yerong Ma[4,5], Yinli Zhang[4,5], Hanqi Ying[4,5], Xiaomei Tong[4,5], Weijie Yang[4,5], Yibin Pan[4,5], Yan Rong[4,5], Yangyang Dai[4,5], Songying Zhang[4,5*] and Peidong Han[1,2,3*]

Abstract

Background Cyclophosphamide (CTX) often induces oocyte and granulosa cell injury, leading to fertility loss in young female cancer survivors. Deciphering the mechanisms underlying follicular cell injury could offer novel insights into fertility preservation. Granulosa cells represent the most abundant cell type within the follicles and can be generally categorized as cumulus granulosa cells (CGCs) and mural granulosa cells (MGCs). Despite the essential roles of granulosa cells in supporting ovarian function in physiological conditions, their distinct lineage-specific responses to CTX remains elusive.

Results Here, we performed a genome-wide transcriptome analysis of murine mural and cumulus granulosa cells before and after CTX administration. Compared with MGCs, CGCs exhibited higher basal mammalian target of rapamycin (mTOR) activity and an increased DNA damage response post-injury. Pharmacological mTOR suppression or RNA interference-mediated gene silencing of Raptor, a key component of the mTORC1 complex, significantly reduced DNA damage in granulosa cells induced by 4-HC, an activated form of CTX. Notably, by examining human granulosa cells in response to 4-HC, our results uncovered a conserved role of mTOR inhibition in ovarian protection.

Conclusions Taken together, our findings reveal that intrinsic variations in mTOR activity in CGC and MGC lineages determine their differential responses to CTX. Targeting this signaling pathway may prove beneficial in mitigating CTX-induced granulosa cell apoptosis and protecting against ovarian injury.

Keywords Granulosa cells, Apoptosis, DNA damage response, mTOR signaling pathway, Cyclophosphamide

*Correspondence:
Songying Zhang
zhangsongying@zju.edu.cn
Peidong Han
hanpd@zju.edu.cn
[1]Department of Cardiology, Center for Genetic Medicine, the Fourth Affiliated Hospital, Zhejiang University School of Medicine, Yiwu, China
[2]Institute of Genetics, Zhejiang University International School of Medicine, Hangzhou, Zhejiang, China
[3]Zhejiang Provincial Key Laboratory of Genetic & Developmental Disorders, Hangzhou, Zhejiang, China
[4]Assisted Reproduction Unit, Department of Obstetrics and Gynecology, Sir Run Run Shaw Hospital, Zhejiang University School of Medicine, Hangzhou, China
[5]Zhejiang Key Laboratory of Precise Protection and Promotion of Fertility, Hangzhou, China

Introduction

The advancement in the diagnosis and treatment of malignant tumors, particularly chemotherapy, has significantly elevated the survival rates among young cancer patients [1, 2]. Cyclophosphamide (CTX), an alkylating anticancer drug, is commonly used in the treatment of various malignant tumors [3]. However, its use is associated with the potential for ovarian damage, posing a significant threat to fertility in young female cancer survivors [4, 5]. A growing body of evidence demonstrates that, during ovarian injury, primordial and growing follicles are adversely affected through diverse mechanisms [6–8]. Specifically, CTX promotes excessive activation and direct loss of primordial follicles, diminishing ovarian reserves and leading to long-term premature ovarian insufficiency [9–14]. In contrast, in the case of mature follicles, CTX promotes DNA double strand breaks and the apoptosis of oocytes and their surrounding granulosa cells, resulting in irreversible ovarian damage [6, 12]. Thus, preventing CTX-induced ovarian injury is crucial to mitigate the gonadotoxic effects.

The oocytes and the surrounding granulosa cells collectively form the majority of the cell mass within follicles of mice. Granulosa cells are stratified cubic epithelial cells that are essential for folliculogenesis and maintaining a normal menstrual cycle under physiological conditions [15, 16]. Instead of constituting a homogenous population, these cells exhibit spatial and functional heterogeneity [17]. Throughout follicle development, preantral granulosa precursor cells gradually differentiate into two sub-populations: mural cells lining the follicle wall and cumulus cells residing in close proximity to the oocytes [18]. These two groups of cells display unique gene expression profiles [16] and perform specialized functions, including contributing to steroidogenesis (mural cells) and promoting oocyte maturation via paracrine factors (cumulus cells) [19].

Given the important roles played by granulosa cells in maintaining proper ovarian function, stress-induced apoptosis in these cells often leads to follicle atresia and fertility dysfunction. During in vitro fertilization (IVF), granulosa cell apoptosis correlates with a low proportion of healthy follicles, a poor pregnancy rate, and a decreased live birth rate [20]. Likewise, the administration of CTX induces substantial granulosa cell apoptosis and temporary amenorrhea [12, 21]. Interestingly, the patterns of granulosa cell apoptosis occur in a context-dependent manner. For instance, previous studies have demonstrated that apoptosis initiates from inner mural granulosa cells during programed follicle atresia [20, 22]. In contrast, human preovulatory follicles show an enrichment of antiapoptotic proteins in mural cells [23]. These observations underscore the importance of the intrinsic characteristics of mural and cumulus cells in determining their distinct responses to stress signals. While granulosa cell injury has been implicated in chemotherapy-induced ovarian damage, our current understanding of the potentially distinct roles played by mural and cumulus cells in this process remains limited. Consequently, a comprehensive understanding of the molecular mechanisms underlying ovarian injury is crucial for developing effective therapeutic strategies.

To determine intrinsic differences in gene expression profiles between MGCs and CGCs, as well as their distinct responses to CTX, we applied transcriptome analysis on purified MGCs and CGCs collected from mice before and after CTX treatment. Before CTX administration, we found an enrichment in genes associated with the mTOR signaling pathway in CGCs compared to MGCs. Intriguingly, our results revealed that DNA damage response-related genes were specifically enriched in CGCs, but not in MGCs, following CTX treatment. Pharmacological inhibition of mTOR using RAD001 or genetic knockdown of Raptor significantly reduced DNA damage and ameliorated CTX-induced cell death in CGCs. Notably, this molecular mechanism uncovered in animal model was conserved in human granulosa cells. Overall, our findings provide compelling evidence that CGCs are predisposed to DNA damage and cell injury through endogenous mTOR activity. Targeting this signaling pathway may offer a promising strategy for preserving fertility in young female cancer patients.

Materials and methods

Animals

ICR female mice (7–8 weeks old, 25 g) were obtained from Beijing Vital River Laboratory Animal Technology. Animals were housed under standard laboratory conditions in an environmentally controlled room and treated in accordance with the Animal Research Committee guidelines of Zhejiang University. To induce chemotherapeutic injury in ovaries, mice were treated with a single injection of CTX (150 mg/kg) (Endoxan, Baxter Oncology GmbH) [24–26], after 24 h, ovaries were collected and subjected to further analysis. To investigate the effect of mTOR signaling pathway inhibition on CTX-induced granulosa cell injury, mice were subjected to daily intraperitoneal injection of RAD001 (2.5 mg/kg, Selleck, S1120) for a week as reported previously [21, 27, 28], then were treated with CTX as described above.

Antibodies

The primary antibodies used in this study include: anti-Phospho-Histone H2A.X (Ser139) (9718 S; 1:500 (IF); 1:1000 (WB)), anti-Cleaved Caspase-3 (Asp175) (9661 S; 1:500 (IF); 1:1000 (WB)), anti-Phospho-S6 Ribosomal Protein (Ser235/236) (2211 S; 1:800 (IF); 1:1000 (WB)), anti-Raptor (2280; 1:1000 (WB)) that were obtained from

Cell Signaling Technology. Anti-FOXL2 (ab5096; 1:200 (IF)) antibody was purchased from Abcam. Anti-Chk2 (BS4043; 1:100 (IHC)) antibody was obtained from Bioworlde. Anti-GAPDH (AC033; 1:5000 (WB)), anti-β-actin (AC038; 1:5000 (WB)) were obtained from ABclonal. Anti-Beta Tubulin (10094-1-AP; 1:1000 (WB)) was purchased from Proteintech. The following secondary antibodies were used: Donkey anti-Goat 488 (34316ES60; 1:200; Yeasen), Goat anti-Rabbit 555 (A21428; 1:800; Invitrogen), Goat anti-Rabbit HRP (31430; 1:5000; Invitrogen), Goat anti-Mouse HRP (31460; Invitrogen).

Human samples

Patients with fallopian tubal sterility were recruited from in vitro fertilization (IVF) laboratories at the Sir Run Run Shaw Hospital, Hangzhou, Zhejiang, China. The age of the patients was 28.9±4.61 years, and the ovarian stimulation protocol was ultra long GnRH agonist. All recruited patients signed informed consent forms, and all experimental procedures were approved by Sir Run Run Shaw Hospital Ethics Committee (20210319-32). Cumulus cells and mural cells were aspirated from the patients during oocyte retrieval. CGCs were mechanically isolated by cutting the cumulus layer of each leading oocyte and washed twice with phosphate-buffered saline (PBS). The mural cells presented as clumps under a stereoscope were removed with a glass pipet and isolated from follicular fluid by density gradient centrifugation using percoll (P8370, Solarbio). Cells were cultured in DMEM/F12 medium (Meilun) with 10% Fetal Bovine Serum (FBS, Vistech) and 1% (v/v) penicillin and streptomycin (Meilunbio).

Isolation of mural and cumulus granulosa cells

Mural and cumulus granulosa cells were separated and collected as described previously [29, 30]. Briefly, ICR mice were given a single intraperitoneal injection of 5 IU pregnant mare serum gonadotrophin (PMSG, Ningbo Sansheng Pharmaceutical), after 24 h, chemotherapeutic injury was induced in CTX group and control group was treated with PBS. Another 24 h after administration of CTX, ovaries from multiple mice were collected and washed in PBS. Multiple fully grown follicles were dissociated using 29G needles. The cumulus granulosa cells were collected following microsurgical oocytectomy. The mural granulosa cells characterized as clumps under stereomicroscope were separated with glass pipet.

Collection and culture of primary granulosa cells

As described previously, ICR mice was superovulated by 5 IU PMSG for 44 h and ovaries was harvested into PBS for collecting granulosa cells [31]. Isolated granulosa cells were cultured in DMEM/F12 medium (Meilun) with 10% FBS (Vistech) and 1% (v/v) penicillin and streptomycin (Meilunbio).

Small molecule treatment

RAD001 was purchased from Selleck (S1120) and mixed with DMSO (D2650, Sigma), which was further diluted with PBS to obtain 10 μM stock solution. A same amount of DMSO diluted with PBS was used as control. Subsequently, RAD001 stock solution or control solution was further diluted with DMEM/F12 medium (Meilun) with 10% FBS (Vistech). For in vitro experiments, human or mouse MGCs and CGCs were treated with PBS (control), or 100 nM RAD001 for 24 h. Subsequently, cells were exposed to 3 μM 4-HC (Santa, sc-206885 A) for another 24 h before collected for further analysis.

Histology and Immunofluorescence

Ovaries were fixed in 4% paraformaldehyde overnight and equilibrated through 15% and then 30% sucrose in PBS solution, before embedded and frozen in O.C.T. compound (Sakura). 7 μm cryosections were prepared on a cryostat. Cells or tissue sections were incubated in PBS solution containing 5% bovine serum albumin (BSA) and 0.3% Triton X-100 for 1 h at room temperature. Samples were then incubated overnight with primary antibodies at 4℃, followed by incubation for 1 h with corresponding secondary antibodies at room temperature. Nuclei were stained with DAPI. Apoptosis in mouse ovaries were determined using terminal deoxynucleotidyl transferase-mediated dUTP nick end-labeling (TUNEL) with an in situ cell death detection kit (Yeasen) according to the manufacturer's instructions. Fluorescent images were obtained using a Nikon C2 confocal microscope and analyzed with ImageJ software.

RNA interference-mediated gene Silencing

The si-Raptor and negative control siRNAs were synthesized by Genepharma Company (Shanghai, China). All siRNA transfections were performed with Lipofectamine RNAiMAX Transfection Reagent (Invitrogen) at 30 pM final concentration according to the manufacturer's protocol. The si-Raptor sequences was 5'- CUCCCUCAUA GGAGUUUCUTT-3'; and the negative control sequence for si-Raptor was 5'- AGAAACUCCUAUGAGGGAGT T-3'.

Western blot analysis

Granulosa cells were homogenized in RIPA buffer (Beyotime) with protease inhibitors (Sangon Biotech) and phosphatase inhibitors (Sangon Biotech). The protein loading concentration was 10 ug for CGCs and MGCs, and 30 ug for cultured primary granulosa cells. Proteins were separated by SDS-polyacrylamide gel electrophoresis and transferred to PVDF membranes. Next, the

membranes were incubated in 5% BSA/TBST for 1 h at room temperature, followed by incubation at 4 °C overnight with primary antibodies diluted in 5% BSA/TBST. After washing three times in TBST, the membranes were incubated at room temperature for 1 h with horseradish peroxidase conjugated secondary antibodies. After washing three times in TBST, the membranes were visualized with chemiluminescence (Thermo Fisher Scientific). ImageJ software was used to quantify the intensities of the western blot bands.

Quantitative real-time PCR analysis

Total RNA was isolated using the RNeasy Plus Micro Kit (74034, Qiagen) and 200 ng total RNA was used for the reverse transcription transcription using PrimeScript RT Master Mix (Takara). Quantitative real-time PCR was performed using SYBR Green Master Mix (Takara) in a CFX96 Real-time PCR detection system. The primer sets used for quantitative real-time PCR analysis were obtained from Primer Bank database (https://pga.mgh.harvard.edu/primerbank/) and listed in Supplementary Table 1. Melting curve analysis was performed at the end of each run to ensure a single amplicon. The expression of individual gene was normalized to the level of *Gapdh*, then compared with the control group. Unpaired two-tailed Student's t-test and one-way ANOVA were used to determine statistical significance between groups. All samples were tested for normality before ANOVA. $^{*}P < 0.05$; $^{**}P < 0.01$; $^{***}P < 0.001$. No statistical method was used to predetermine sample size.

RNA-seq library preparation and data analysis

Cumulus granulosa cells and mural granulosa cells were collected as previously described [21]. Total RNA was isolated using the RNeasy Plus Micro Kit (74034, Qiagen) according to the manufacturer's protocol. The total amount of RNA extracted was 200 ng. Purified cDNA from previous steps was fragmented into small pieces with fragment buffer by PCR, and the product was purified and selected by the Agencourt AMPure XP-Medium kit (Thermo Fisher Scientific, USA). The double stranded PCR product undergo QC step was heat denatured and circularized by the splint oligo sequence. The single strand circle DNA (ssCir DNA) was formatted as the final library. The final library was amplified with phi29 (Thermo Fisher Scientific) to make DNA nanoball (DNB) which had more than 300 copies of one molecular, DNBs were loaded into the patterned nanoarray and single end 50 bases reads were generated on BGISEQ500 platform(BGI-Shenzhen, China). All analysis was performed using the PossionDis with False Dicovery Rate (FDR) < 0.05 and|Log2Ratio| >1. To take insight to the change of phenotype, GO and KEGG enrichment analysis of annotated different expressed gene was performed by Phyper based on Hypergeometric test. The significant levels of terms and pathways were corrected by Q value with a rigorous threshold (Q value < 0.05) by Bonferroni. Two independent experiments were repeated for each group.

Image processing statistical analysis

All images were obtained under the same parameters and processed using Nikon NIS elements software or ImageJ. Statistical analysis was performed using GraphPad Prism software version 8.0 (GraphPad Software, Inc).

Statistical analysis

Data are presented as mean ± s.e.m. Unpaired two-tailed Student's t-test and one-way ANOVA were used to determine statistical significance between groups. All samples were tested for normality before ANOVA. $^{*}P < 0.05$; $^{**}P < 0.01$; $^{***}P < 0.001$. No statistical method was used to predetermine sample size.

Results

Lineage-specific responses of granulosa cells to chemotherapeutic injury

To examine the responses of granulosa cells to genotoxic chemotherapy, we used a CTX-induced ovary injury animal model, as previously reported [24, 25, 32, 33]. Twenty-four hours after intraperitoneal CTX injection (150 mg/kg), mouse ovaries were collected for further examination. Initial immunostaining of Cleaved Caspase3 with Foxl2 (granulosa cell marker) revealed a significantly higher signal of Cleaved Caspase3 after CTX treatment (Fig. 1a, b). Interestingly, Cleaved Caspase3^{+} foci were not uniformly distributed across the entire ovary but were concentrated in the vicinity of the oocyte. Quantitative analysis confirmed an inverse correlation between the proportion of Cleaved Caspase3^{+} granulosa cells and the distance to the oocyte (Fig. 1b, right). Immunohistochemistry analysis further validated the enrichment of Cleaved Caspase3 signals surrounding the oocyte (Fig. 1c). In addition, TUNEL staining, capable

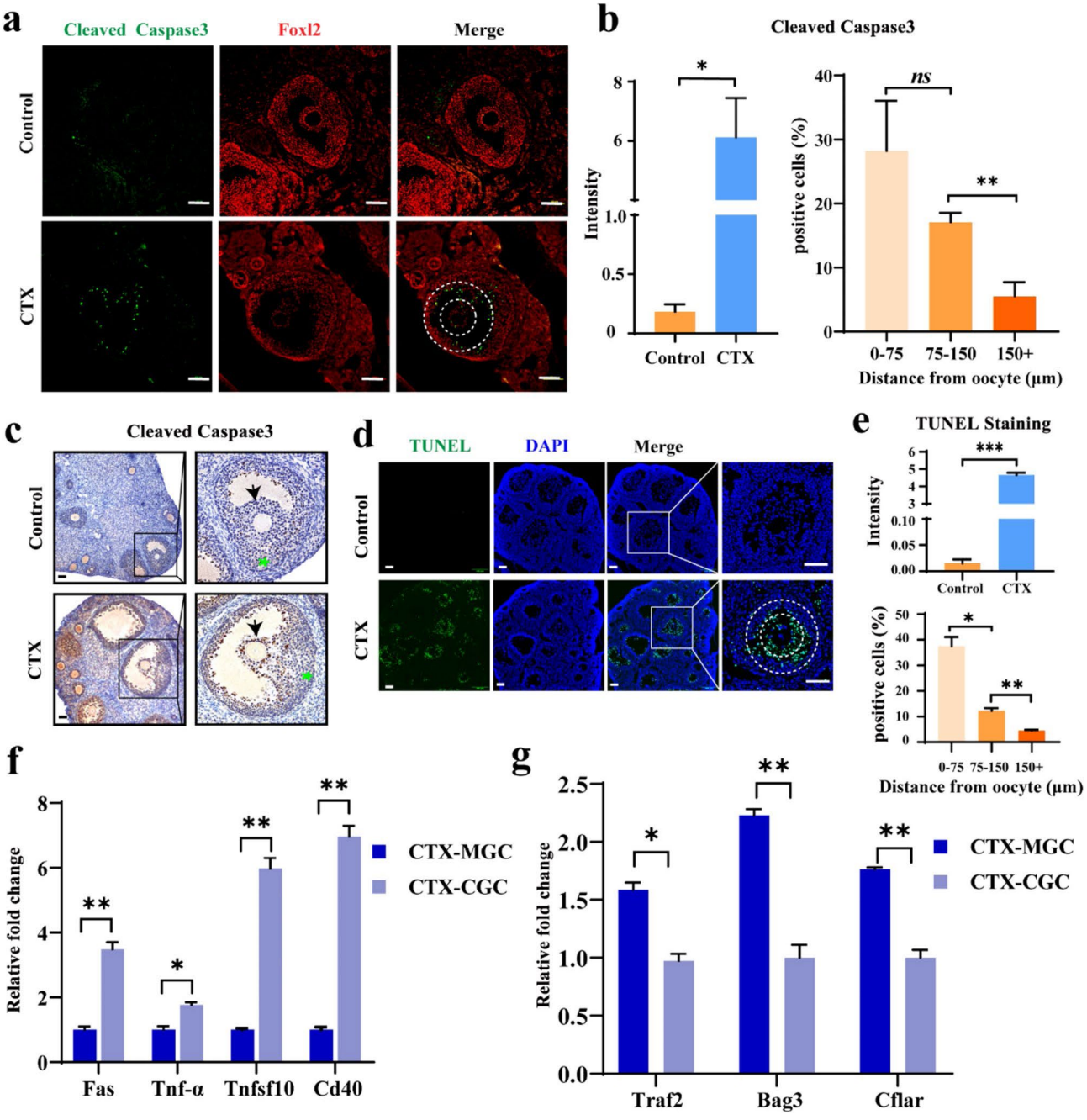

Fig. 1 Cumulus granulosa cells are more susceptible to chemotherapeutic injury. (**a**) Representative immunostaining images of Cleaved Caspase3 (green) and Foxl2 (granulosa cell marker, red) on antral follicles from mice subjected to PBS (control) or 150 mg/kg CTX treatment. The middle of the dashed circles represents the oocyte; the radius of the inner and outer circles are 75 μm and 150 μm, respectively. (**b**) Quantitative analysis shows the immunofluorescence intensity of Cleaved Caspase3 (left) and the inverse correlation between the proportion of Cleaved Caspase3 positive cells and their distance to the oocyte (right). (**c**) Immunohistochemistry analysis of Cleaved Caspase3. Square box: follicle; Arrows: cumulus-cell-oocyte complex; Asterisks: mural granulosa cells. (**d**) TUNEL staining (green) shows cells undergoing apoptosis, nuclei are stained with DAPI. The radius of the inner and outer circles are 75 μm and 150 μm, respectively. Square box: follicle. (**e**) Quantitative analysis shows the intensity of TUNEL staining (top) and the inverse correlation between the proportion of TUNEL positive cells and their distance to the oocyte (bottom). (**f**) Quantitative real-time PCR analysis shows the expression levels of *Fas*, *Tnf-α*, *Tnfsf10* and *Cd40* in MGCs and CGCs. (**g**) The expression levels of *Bag3*, *Traf2*, and *Cflar* in MGCs and CGCs. $N = 3–6$ mice per group. Scale bar, 100 μm. All data are shown as mean ± s.e.m. *ns*, not significant; $^{*}P < 0.05$, $^{**}P < 0.01$ and $^{***}P < 0.001$

of detecting late-stage apoptotic cells undergoing extensive DNA degradation, displayed increased fluorescence intensity and a similar allocation pattern in CTX-treated follicles (Fig. 1d, e).

Considering that apoptotic cells are more likely to appear where CGCs reside, we hypothesized that CGCs undergo more severe injury after CTX treatment compared to MGCs. To validate this hypothesis, CGCs and MGCs were isolated and purified using a previously published protocol [34]. The identity of the cells was confirmed by expression analysis of the genes *Amh* and *Lhcgr*, recognized markers for CGCs and MGCs, respectively (Supplementary Fig. 1a). In agreement with results from immunostaining assays, qPCR analysis revealed increased expression levels of genes such as *Fas*, *Tnf-α*, *Tnfsf10* and *cd40* in CGCs compared to MGCs (Fig. 1f), suggesting an enhanced apoptotic index in CGCs. In support of this observation, the anti-apoptosis markers *Bag3*, *Traf2* and *Clfar* were decreased in CGCs (Fig. 1g). Altogether, these results indicate CGCs are more susceptible to CTX-induced injury compared to MGCs.

CGCs and MGCs exhibit distinct mTOR activity under basal physiological conditions

To determine whether the distinct responses to genotoxic chemotherapy in CGCs and MGCs result from their unique gene expression profiles, we performed RNA-seq on purified CGCs and MGCs collected from wild-type mouse ovaries. Transcriptome analysis identified 413 down-regulated and 371 up-regulated genes in CGCs compared to MGCs (Fig. 2a). In addition, KEGG pathway analysis showed that genes with significantly higher expression levels in CGCs were enriched in Rap1, GnRH signaling pathway, Ras, Thyroid hormone, and PI3K-Akt signaling pathways (Fig. 2b). In particular, the PI3K-Akt signaling pathway contained the highest number of candidate genes, in agreement with a previous study showing the essential role of the PI3K-Akt-mTOR axis in chemotherapy-induced ovarian injury [9, 10]. Gene set enrichment analysis unveiled increased expression levels of several mTOR signaling components, including *Map2k1*, *Wdr59*, *Lrp5*, *Lrp6*, *Slc7a5*, and *Igf1r*, in CGCs (Fig. 2c). qRT-PCR results further confirmed these findings (Fig. 2d). Because ribosomal S6 (Rps6) is a key downstream signaling mediator for mTOR activity, we examined its mRNA abundance and found higher expression levels in CGCs (Fig. 2d). Similarly, immunofluorescence results showed markedly stronger staining of phosphorylated (p-Rps6) in CGCs compared to neighboring MGCs (67.4% vs. 33.6%, $P < 0.01$) (Fig. 2e, f). In support of these findings, western blot analysis detected greater levels of p-Rps6 in CGCs (Fig. 2g, h). Overall, our findings indicate that CGCs exhibit elevated mTOR activity compared to MGCs under basal physiological conditions.

Distinct DNA damage responses of CGCs and MGCs underlie ovarian injury

To investigate the underlying mechanisms behind the observed differential apoptosis rate observed in CGCs and MGCs during ovarian injury, we performed RNA-seq on purified granulosa cells collected from CTX treated mouse ovaries. In total, we identified 683 down-regulated and 1788 up-regulated genes in CGCs compared to MGCs (Fig. 3a). KEGG analysis showed the enrichment of pathways related to DNA damage response, including fanconi anemia, mismatch repair, p53 signaling, non-homologous end-joining, and base excision repair pathways (Fig. 3b). Using γ-H2A.X and Phospho-Chk2 as markers for DNA damage, we observed a higher proportion of positively stained CGCs compared to MGCs (Fig. 3c-f). Western blot analysis also detected increased γ-H2A.X in purified CGCs (Fig. 3g).

Pharmacological inhibition of the mTOR signaling pathway ameliorates damage of granulosa cells

The mTOR signaling pathway has been previously recognized for its potential to impair DNA damage response [35]. Reasoning that higher mTOR activity in CGCs may lead to enhanced apoptosis following CTX treatment, we treated cultured mouse granulosa cells with the mTORC1 inhibitor everolimus (RAD001) to determine whether mTOR suppression could elicit a protective effect against CTX-induced injury. RAD001 specifically blocks S6K1 activation and subsequent phosphorylation of Rps6. After 24 h of treatment, both immunofluorescence and western blot results showed a substantial decrease in p-Rps6, indicating efficient inhibition of mTOR activity (Fig. 4a, d, e). In addition, a significantly reduced proportion of γ-H2AX$^+$ granulosa cells was observed in the

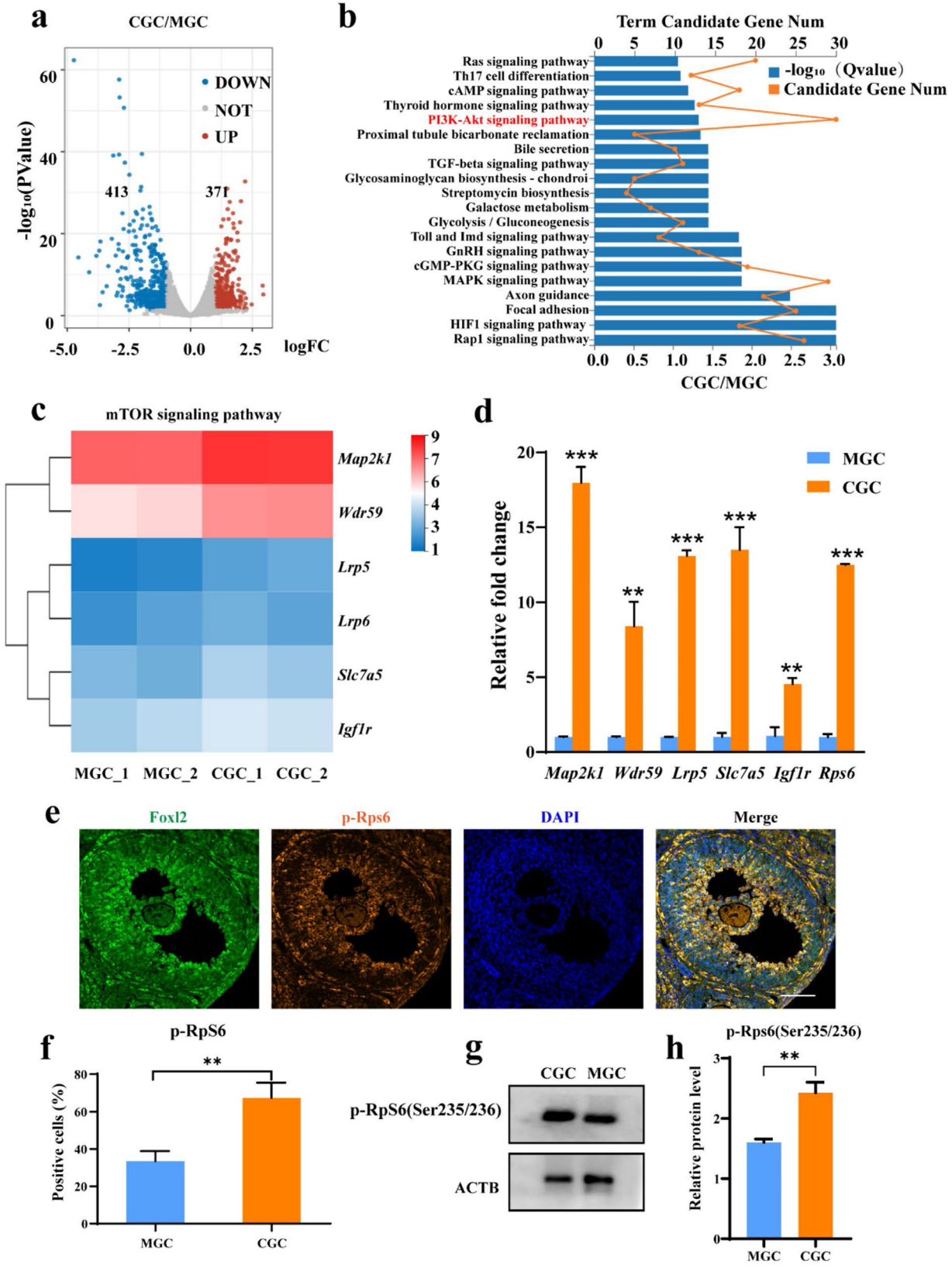

Fig. 2 (See legend on next page.)

(See figure on previous page.)

Fig. 2 Differential gene expression profiles and mTOR activity in CGCs and MGCs. (**a**) Volcano plot shows gene expression changes between CGCs and MGCs isolated from wild-type mice. Genes with a fold change > 1.5 or < 2/3 and an adjusted *P* value < 0.05 were considered as significantly up-regulated (red) or down-regulated (blue), respectively. *N* = 45 mice. The experiment was independently performed twice. (**b**) KEGG pathway analysis of the enriched pathways associated with differentially expressed genes in CGCs compared with MGCs from wild-type ovaries. (**c**) Heatmap shows the relative expression of genes related to the mTOR pathway. (**d**) Quantitative real-time PCR analysis shows the relative mRNA levels of genes related to the mTOR pathway in MGCs and CGCs. (**e**) Phosphorylated Rps6 (p-Rps6, yellow) and Foxl2 (green) immunostaining of follicles. (**f**) Quantification of the p-Rps6 positive cells in MGCs and CGCs. *N* = 9 sections from 3 independent experiments. (**g**) Protein expression levels of p-Rps6 in MGCs and CGCs. (**h**) Quantification of protein expression of p-Rps6. Scale bar, 100 μm. All data are shown as mean ± s.e.m. Unpaired two-tailed Student's t-test was used to determine statistical significance between groups. ***P* < 0.01, ****P* < 0.001

RAD001 treated group (Fig. 4b, c, e), indicative of a lower DNA damage rate.

Likewise, we determined the effects of inhibiting mTOR in vivo. Compared to mice receiving CTX alone, animals injected with RAD001 and CTX exhibited a dramatic decrease in p-Rps6 fluorescence intensity in granulosa cells (Fig. 4f, g). Furthermore, we observed a reduced proportion of granulosa cells with γ-H2AX$^+$ staining, which also displayed lower fluorescence intensity in ovaries with mTOR inhibition (Fig. 4h, i). Collectively, these results indicate that the inhibition of mTOR activity exerts a protective effect against DNA damage and apoptosis.

Genetic knockdown of *Raptor* recapitulates the protection effect of the mTOR inhibitor

To further substantiate that mTOR inhibition protects against CTX-induced granulosa cell injury, we performed RNA interference-mediated gene silencing in cultured mouse granulosa cells to knock down *Raptor*, the key component of the mTORC1 complex. Western blot confirmed the downregulation of *Raptor* in cells transfected with siRNA compared to scramble siRNA (siNC) (Fig. 5a, b). As expected, *Raptor* knockdown caused a substantial downregulation of p-p70s6k and p-Rps6 (Fig. 5a, b), indicating the inactivation of mTOR signaling. As CTX requires hepatic metabolism to generate active metabolites, our in vitro studies utilized one of its active metabolites, specifically 4-Hydroperoxy cyclophosphamide (4-HC). After exposure to 4-HC, immunofluorescence results further demonstrated reduced staining of p-Rps6 in Raptor siRNA-treated granulosa cells compared to cells receiving scramble siRNA (Supplementary Fig. 2). Consistently, the knockdown of Raptor resulted in diminished γ-H2AX$^+$ granulosa cells after 4-HC exposure (Fig. 5a-d), corroborating the protective effects of mTOR inhibition.

Lineage-specific mTOR activity is conserved in human granulosa cells

To assess the conservation of our findings in animal models within the human context, we performed experiments on human CGCs and MGCs isolated using a previously reported method [36]. The identity of these cells were confirmed through gene expression analysis of AMH and LHCGR (Supplementary Fig. 1b). By analyzing genes associated with the mTOR signaling pathway, we discovered elevated expression levels of *MAP2K1*, *WDR59*, *LRP5*, *SLC7A5*, and *IGF1* in CGCs compared to MGCs (Fig. 6a). Immunostaining further indicated a higher proportion of p-Rps6$^+$ CGCs compare to MGCs (Fig. 6b), consistent with the previously obtained results from mouse granulosa cells.

We next employed 4-HC treatment on human CGCs and MGCs to explore the differential expression of DNA damage-related genes. Quantitative real-time PCR analysis showed higher expression levels of the genes *TOP3A* and *FAAP100* in CGCs (Fig. 6c), suggesting the activation of the fanconi anemia pathway. Similarly, we detected an enhanced expression of *SESN2* and *THBS1* (Fig. 6c), both of which are P53 signaling pathway markers. These data suggest that, during chemotherapeutic drug treatment, human CGCs are more susceptible to DNA damage than MGCs. Consistently, a higher proportion of CGCs were γ-H2AX$^+$ (Fig. 6d). Taken together, our results suggest that the differential mTOR activity and DNA damage responses observed in MGCs and CGCs in animal models are conserved in human granulosa cell lineages.

mTOR Inhibition in human granulosa cells protects against CTX-induced injury

To elucidate the role of mTOR inhibition in human granulosa cell injury, isolated MGCs and CGCs were exposed to PBS (control) or RAD001 for 24 h. Subsequently, these cells were treated with PBS or 4-HC for an additional

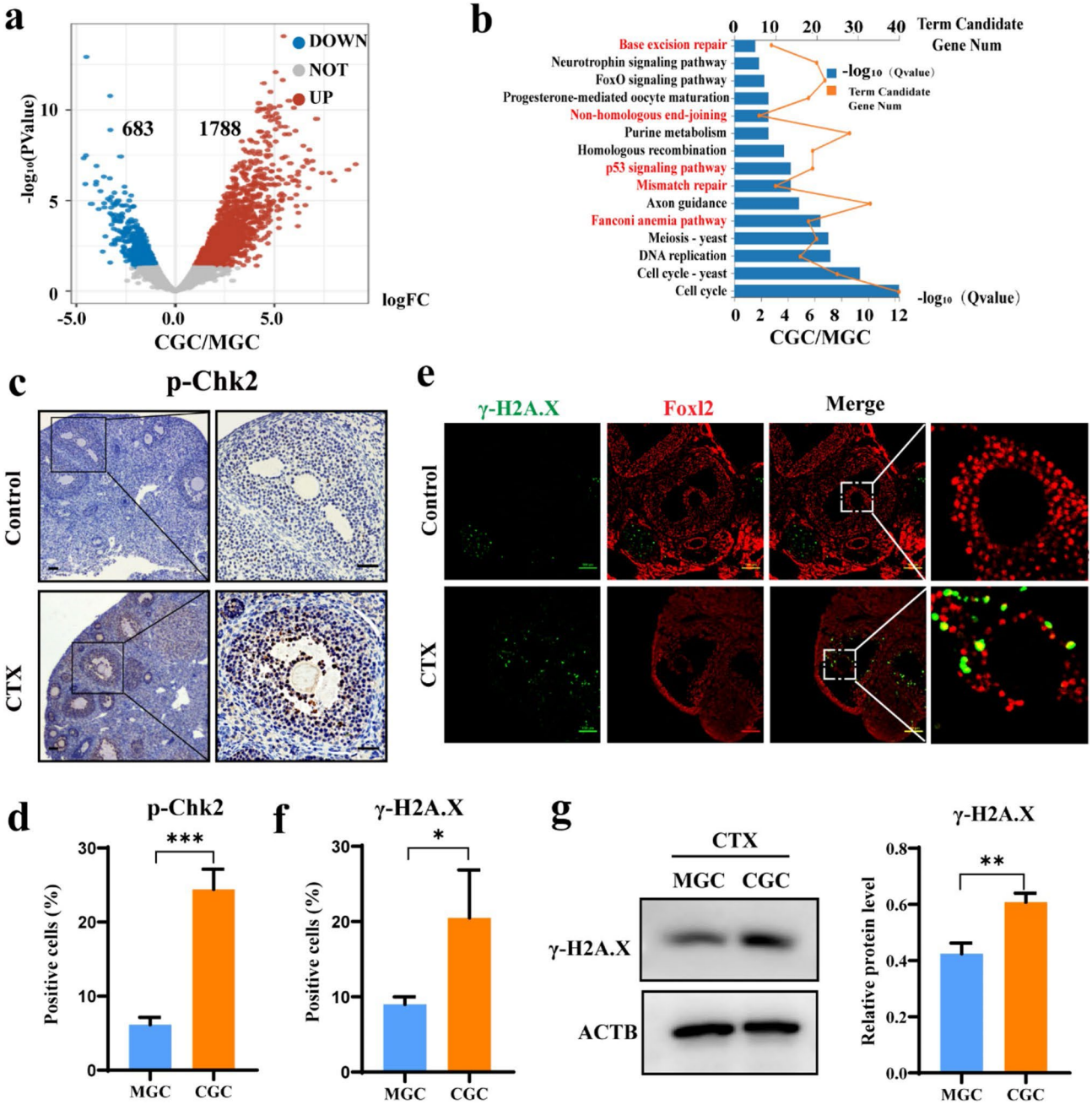

Fig. 3 CGCs and MGCs exhibit distinct DNA damage responses during ovarian injury. (**a**) Volcano plot shows gene expression changes between CGCs and MGCs isolated from CTX-treated mice. Genes with a fold change > 1.5 or < 2/3 and an adjusted *P* value < 0.05 were considered as significantly up-regulated (red) or down-regulated (blue), respectively. *N* = 60 mice. The experiment was independently performed twice (**b**) KEGG pathway analysis of the enriched pathways associated with differentially expressed genes in CGCs compared with MGCs from ovaries receiving CTX-treatment. (**c**) Immunohistochemistry of phosphorylated Chk2 (p-Chk2). Representative images are based on *N* = 6 mice per group. (**d**) Quantification of p-Chk2 on control or CTX treated follicles. (**e**) Representative images of γ-H2A.X (green) and Foxl2 (red) immunostaining on control or CTX treated follicles. (**f**) Percentages of γ-H2A.X positive cells in CGCs and MGCs in CTX treated follicles. (**g**) Western blot and quantification of γ-H2A.X in CGCs and MGCs isolated from CTX-treated mice. *N* = 20 mice. Three independent experiments were performed. Scale bar, 50 μm. All data are shown as mean ± s.e.m.**P* < 0.05. ***P* < 0.01, ****P* < 0.001

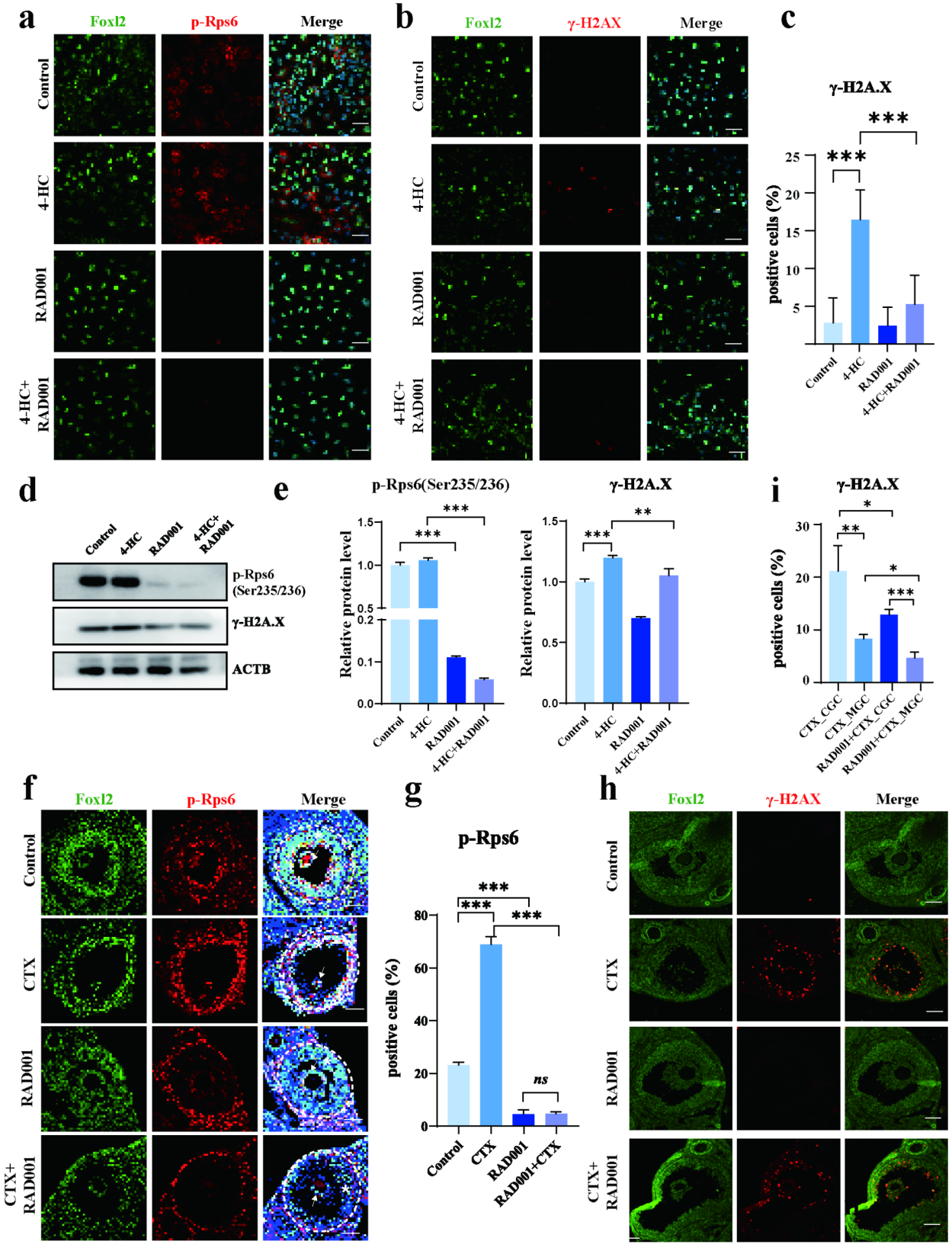

Fig. 4 (See legend on next page.)

(See figure on previous page.)

Fig. 4 mTOR inhibition ameliorates CTX-induced DNA damage in granulosa cells. (**a**, **b**) Isolated granulosa cells were treated with PBS (control), RAD001, 4-HC or 4-HC and RAD001. After 24 h, immunostaining was performed to detect p-Rps6 (**a**) or γ-H2A.X (**b**). $N = 15$ mice for each condition. Three independent experiments were performed. (**c**) Statistical analysis of the percentages of γ-H2A.X positive cells at indicated conditions. (**d**) Western blot shows the expression of p-Rps6 and γ-H2A.X in granulosa cells at indicated conditions. (**e**) Quantification of the protein expression levels of p-Rps6 and γ-H2A.X. (**f-i**) Mice were treated with PBS (control), RAD001, CTX or CTX and RAD001. Ovaries were collected and subjected to p-Rps6 (**f**) or γ-H2A.X (**h**) immunostaining. White dotted circle: granulosa cells in a follicle; Arrows: cumulus-cell-oocyte complex; Asterisks: mural granulosa cells. Quantification of the percentages of p-Rps6 (**g**) and γ-H2A.X (**i**) positive cells. $N = 6$ mice for each condition. Three independent experiments were performed. Scale bar, 50 μm. All data are shown as mean ± s.e.m. *ns*, not significant, $^{*}P < 0.05$, $^{**}P < 0.01$, and $^{***}P < 0.001$

24 h. As expected, mTOR inhibition resulted in diminished p-Rps6 expression (Supplementary Fig. 3). Immunofluorescence staining detected a significantly lower proportion of γ-H2A.X^{+} CGCs with RAD001 treatment (Fig. 7a, b), confirming the conserved protective role of mTOR inhibition against CTX injury in human cells.

Discussion

The impact of chemotherapeutic drugs on ovarian function, particularly CTX-induced ovarian injury, is a significant contributor to fertility loss in young female cancer survivors. CTX causes DNA damage and frequent cell death in oocytes and surrounding granulosa cells, resulting in irreversible ovarian damage and a substantial negative impact on female fertility [4]. To develop effective therapeutic strategies for fertility preservation, it is essential to unravel the cellular and molecular mechanisms underlying cell injury within the follicles. Granulosa cells, encompassing both CGCs and MGCs, represent a prominent cell population within follicles and play a pivotal role in supporting oocyte development and folliculogenesis. Specifically, CGCs form a close association with the oocyte, promoting its growth and maturation, while MGCs contribute significantly to steroidogenesis [37, 38]. Despite the recognized heterogeneous spatial distribution and functional characteristics, CGCs and MGCs share certain transcripts. During ovary development, cell-cell interactions between the oocyte and granulosa cells influence the establishment of this cellular heterogeneity. For instance, follicle-stimulating hormone (FSH) promotes the expression of *Lhcgr* in MGCs, a pathway that is abrogated by the oocyte [39]. Although a previous study has demonstrated a subset of differentially expressed genes between CGCs and MGCs [17], our current understanding of the expression profiles of granulosa cell subpopulations remains limited. In this study, we implemented a genome-wide transcriptome analysis of purified CGCs and MGCs, uncovering gene sets specifically expressed in these two subpopulations. This provides a valuable resource for further interrogating granulosa cell heterogeneity. In particular, components of the PI3K-Akt-mTOR axis, including *Map2k1*, *Wdr59*, *Lrp5*, *Lrp6*, *Slc7a5*, and *Igf1r*, were found to be exclusively activated in CGCs. Additionally, RT-PCR analysis of genes downstream the mTOR signaling pathway, along with p-Rps6 immunostaining, further confirmed mTOR activity in CGCs. Hence, investigating the mechanisms initiating differential mTOR signaling will be particular intriguing in future studies.

It has been previously reported that inhibiting mTORC1/2 can preserve the ovarian reserve and primordial follicle counts, offering protection to fertility during genotoxic chemotherapy [10, 27]. However, the response of granulosa cells to these extrinsic stimuli has remained unclear. According to our transcriptome analysis, we found that CGCs are more susceptible to DNA damage than MGCs. Specifically, bioinformatics analysis revealed the enrichment of DNA damage response pathways, such as the mismatch repair, fanconi anemia, p53 signaling, base excision repair, and non-homologous end-joining pathways in CGCs. Consistently, a higher proportion of CGCs exhibited γ-H2A.X and Phospho-Chk2 staining. Moreover, we provided genetic and biochemical evidence highlighting the beneficial effects of mTOR inhibition, primarily mediated by protecting against DNA damage in CGCs. Hence, this study provides more precise insights into preventing ovarian injury in patients undergoing chemotherapy. Given the important role of GCs in folliculogenesis, further research is essential to delineate the mechanisms of the mTOR signaling pathway in regulating GCs functions, including metabolic product formation and hormone synthesis. Special focus should be placed on identifying how disrupted mTOR signaling alters communication between oocytes and GCs.

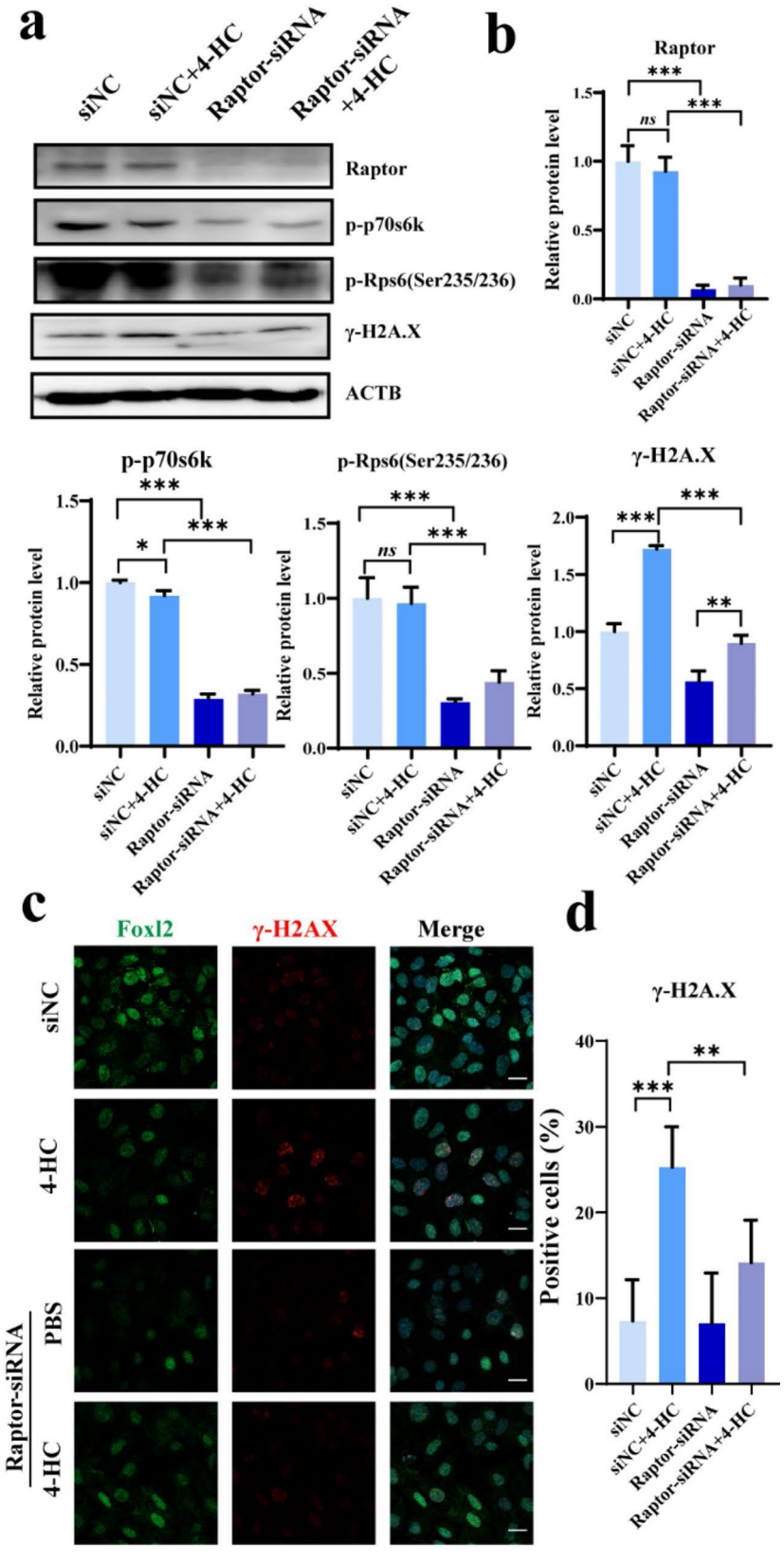

Fig. 5 (See legend on next page.)

(See figure on previous page.)

Fig. 5 Genetic knockdown of *Raptor* protects against CTX-induced DNA damage. (**a**) Granulosa cells were isolated and treated with control siRNA (siNC) or Raptor-siRNA for twenty-four hours, and then exposed to PBS or 4-HC for additional twenty-four hours. Western blot shows the protein expression levels of Raptor, phosphorylated p70 S6 Kinase (p-p70s6k), p-Rps6 and γ-H2A.X at indicated conditions. $N = 20$ mice for each condition. Three independent experiments were performed. (**b**) Quantification of the protein expression levels of Raptor, p-p70s6k, pRps6, and γ-H2A.X. (**c**) γ-H2A.X immunostaining of granulosa cells at indicated conditions. (**d**) Quantification of the percentages of γ-H2A.X positive cells, with a sample size of $N = 15$ mice for each condition. Three independent experiments were performed. Scale bar, 20 μm. All data are shown as mean ± s.e.m. *ns*, not significant, $^{*}P < 0.05$, $^{**}P < 0.01$, and $^{***}P < 0.001$

The mTOR signaling pathway plays an essential role in regulating cell proliferation, growth, metabolism, and survival. CGCs with higher mTOR signaling exhibit increased metabolism and cell proliferation compared to MGCs [28]. Previous study shows that proliferating cells are more vulnerable to DNA damage [40], which may provide a plausible explanation for the increased susceptibility of CGCs to DNA damage. In addition, accumulating evidence suggests a correlation between DNA damage and mTOR signaling [35, 41]. This correlation is particularly intriguing, as CTX treatment often triggers the activation of DNA damage responses. For instance, the fanconi anemia group F protein (FANCD2), a downstream target of the mTOR signaling pathway, can be induced by genotoxic drugs and plays an essential role in maintaining genomic integrity [42]. Consistently, our data also show the activation of the mTOR and fanconi anemia pathways in CGCs, corroborating the crosstalk between the mTOR pathway and DNA damage response. Nevertheless, emphasizing the efficacy of cancer chemotherapy before further exploration of the mTOR signaling as a target for fertility preservation remains challenging.

In summary, through genome-wide transcriptome analysis, pharmacological inhibition and genetic knockdown on a mouse model and human cells, we provide both in vitro and in vivo evidence demonstrating CGCs are inherently predisposed to DNA damage due to intrinsic mTOR activity. Targeting the mTOR signaling

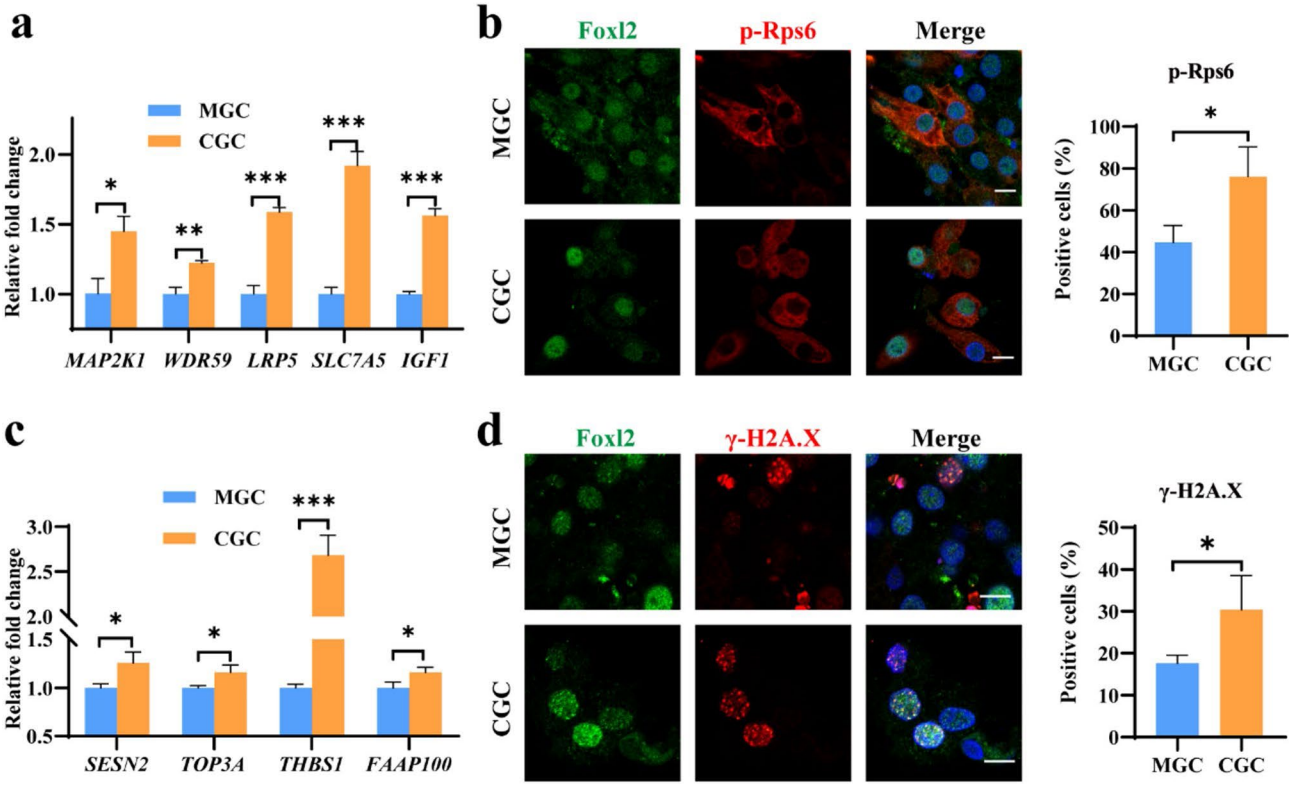

Fig. 6 Human cumulus and mural granulosa cells exhibit distinct mTOR activities. (**a**) Quantitative real-time PCR analysis of isolated human MGCs and CGCs shows the relative mRNA levels of the mTOR pathway related genes, including *MAP2K1*, *WDR59*, *LRP5*, *SLC7A5* and *IGF1*. *GAPDH* serves as internal control. (**b**) Representative immunofluorescence images of p-Rps6 and quantification of the percentage of MGCs and CGCs that are p-Rps6 positive at basal physiological conditions. (**c**) Quantitative real-time PCR analysis shows higher expression of *SESN2*, *TOP3A*, *THBS1* and *FAAP100* in CGCs after 4-HC treatment, suggesting the activation of the fanconi anemia pathway and the P53 signaling pathway. *GAPDH* serves as internal control. (**d**) Immunostaining of γ-H2A.X^{+} human MGCs and CGCs after 4-HC treatment and the quantification results. Human MGCs and CGCs were isolated and cultured for 48 h, before being treated with 3 μM 4-HC or PBS for another 24 h. MGCs and CGCs were isolated from 7 and 10 donors, respectively. Scale bar, 10 μm. All data are shown as mean ± s.e.m. $^{*}P < 0.05$, $^{**}P < 0.01$ and $^{***}P < 0.001$

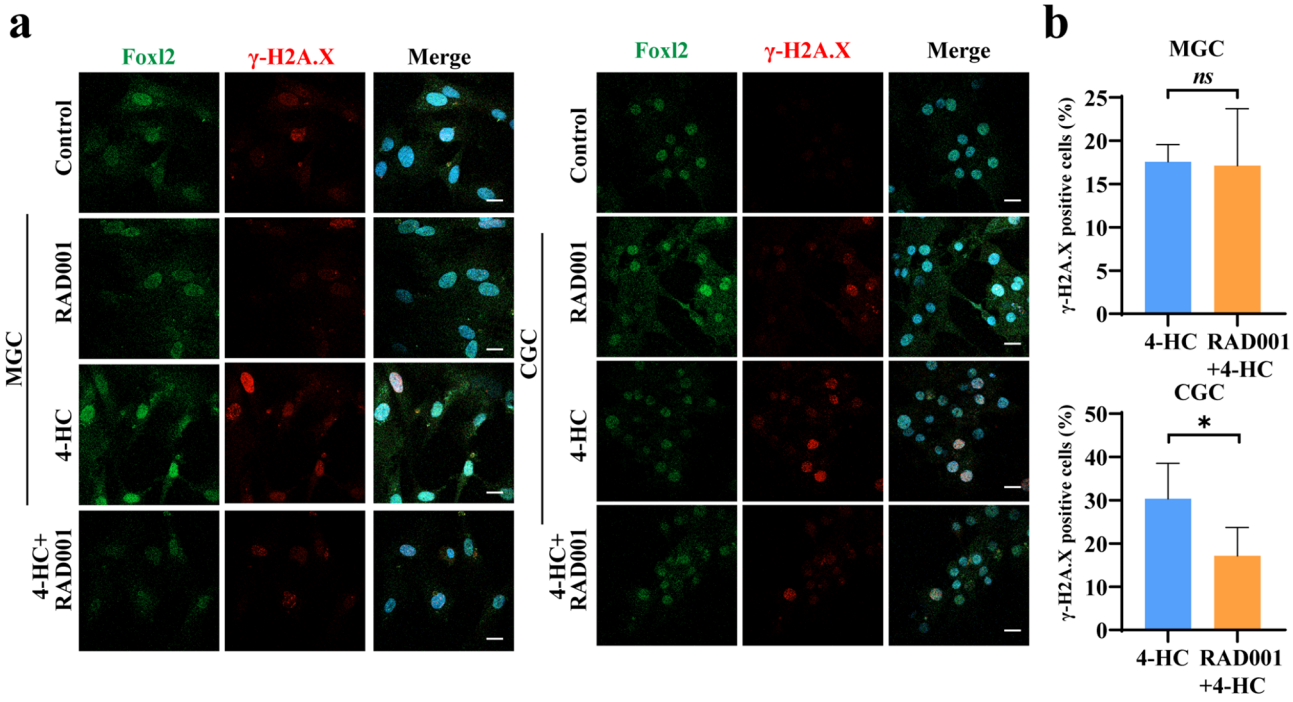

Fig. 7 Conserved function of mTOR inhibition in the protection of human cumulus granulosa cell injury. (**a**) Immunostaining of γ-H2A.X on human MGCs and CGCs treated with PBS (control), RAD001, 4-HC, or 4-HC and RAD001 for 24 h. (**b**) Quantification of the percentages of γ-H2A.X positive cells in MGCs (top) or CGCs (bottom). MGCs and CGCs were isolated from 7 and 10 donors, respectively. Scale bar, 20 μm. All data are shown as mean ± s.e.m. *ns*, not significant. $^{*}P < 0.05$

pathway emerges as a promising strategy to mitigate granulosa cell injury and protect against ovarian injury induced by CTX. Our study thus provides novel insights into safeguarding granulosa cell function and overall ovarian health during chemotherapy.

Supplementary Information

The online version contains supplementary material available at https://doi.org/10.1186/s13048-025-01627-0.

Supplementary Material 1

Supplementary Material 2

Author contributions

Peidong Han and Songying Zhang conceived the project. Peidong Han, Yinli Zhang and Shiqian Xu led the design of the experimental strategy. Xiaomei Tong prepared sample collection. Shiqian Xu, Yerong Ma, Hanqi Ying, Weijie Yang, Yibin Pan, Yan Rong, and Yangyang Dai performed the experiment. Shiqian Xu and Peidong Han prepared the manuscript. All authors contributed to the analysis and interpretation of the data.

Funding

Financial support for this work was provided by National Key Research and Developmental Program of China (2018YFC1004800), and the National Natural Science Foundation of China (32170823, 92468104).

Data availability

The original contributions presented in the study are present in the manuscript and supplementary materials. The RNA-seq data presented in this study was uploaded to the online repositories (https://ngdc.cncb.ac.cn/) and the accession number is PRJCA011448.

Declarations

Ethical approval

The experiment was certified by the ethics committee of Sir Run Run Shaw Hospital affiliated to Zhejiang University, and the number is 20210319-32. All patients signed informed consent regarding the collection of mural granulosa cells and cumulus granulosa cells.

Consent to participate

Not applicable.

Consent for publication

All participants agreed to publication.

Competing interests

The authors declare no competing interests.

Received: 3 July 2024 / Accepted: 14 February 2025
Published online: 11 March 2025

References

1. Allemani C, Weir HK, Carreira H, Harewood R, Spika D, Wang X-S, et al. Global surveillance of cancer survival 1995–2009: analysis of individual data for 25 676 887 patients from 279 population-based registries in 67 countries (CONCORD-2). Lancet. 2015;385:977–1010. https://doi.org/10.1016/S0140-6736(14)62038-9.
2. Xia C, Dong X, Li H, Cao M, Sun D, He S, et al. Cancer statistics in China and united States, 2022: profiles, trends, and determinants. Chin Med J (Engl). 2022;135:584–90. https://doi.org/10.1097/CM9.0000000000002108.
3. Abi Vijenthira J, Kuruvilla M, Crump MJ, Prica A. Cost-Effectiveness analysis of frontline Polatuzumab-Rituximab, cyclophosphamide, doxorubicin, and prednisone and/or Second-Line chimeric antigen receptor T-Cell therapy versus standard of care for treatment of patients with Intermediate- to High-Risk

diffuse large B-Cell lymphoma. J Clin Oncol. 2022;41:1577–90. https://doi.org/10.1200/JCO.22.00478.
4. Sonigo C, Beau I, Binart N, Grynberg M. The impact of chemotherapy on the ovaries: molecular aspects and the prevention of ovarian damage. Int J Mol Sci. 2019. https://doi.org/10.3390/ijms20215342.
5. Spears N, Lopes F, Stefansdottir A, Rossi V, de Felici M, Anderson RA, Klinger FG. Ovarian damage from chemotherapy and current approaches to its protection. Hum Reprod Update. 2019;25:673–93. https://doi.org/10.1093/humupd/dmz027.
6. Matsuda F, Inoue N, Manabe N, Ohkura S. Follicular growth and Atresia in mammalian ovaries: regulation by survival and death of granulosa cells. J Reprod Dev. 2012;58:44–50. https://doi.org/10.1262/jrd.2011-012.
7. Zhang B-F, Hu Y, Liu X, Cheng Z, Lei Y, Liu Y, et al. The role of AKT and FOXO3 in preventing ovarian toxicity induced by cyclophosphamide. PLoS ONE. 2018;13:e0201136. https://doi.org/10.1371/journal.pone.0201136.
8. Ai G, Meng M, Guo J, Li C, Zhu J, Liu L, et al. Adipose-derived stem cells promote the repair of chemotherapy-induced premature ovarian failure by inhibiting granulosa cells apoptosis and senescence. Stem Cell Res Ther. 2023. https://doi.org/10.1186/s13287-023-03297-5.
9. Zhou L, Xie Y, Li S, Liang Y, Qiu Q, Lin H, Zhang Q. Rapamycin prevents cyclophosphamide-induced Over-activation of primordial follicle pool through PI3K/Akt/mTOR signaling pathway in vivo. J Ovarian Res. 2017;10:56. https://doi.org/10.1186/s13048-017-0350-3.
10. Goldman KN, Chenette D, Arju R, Duncan FE, Keefe DL, Grifo JA, Schneider RJ. mTORC1/2 Inhibition preserves ovarian function and fertility during genotoxic chemotherapy. Proc Natl Acad Sci U S A. 2017;114:3186–91. https://doi.org/10.1073/pnas.1617233114.
11. Kalich-Philosoph L, Roness H, Carmely A, Fishel-Bartal M, Ligumsky H, Paglin S, et al. Cyclophosphamide triggers follicle activation and burnout; AS101 prevents follicle loss and preserves fertility. Sci Transl Med. 2013;5:185ra62. https://doi.org/10.1126/scitranslmed.3005402.
12. Ganesan S, Keating AF. The ovarian DNA damage repair response is induced prior to phosphoramide mustard-induced follicle depletion, and ataxia telangiectasia mutated Inhibition prevents PM-induced follicle depletion. Toxicol Appl Pharmacol. 2016;292:65–74. https://doi.org/10.1016/j.taap.2015.12.010.
13. Lande Y, Fisch B, Tsur A, Farhi J, Prag-Rosenberg R, Ben-Haroush A, et al. Short-term exposure of human ovarian follicles to cyclophosphamide metabolites seems to promote follicular activation in vitro. Reprod Biomed Online. 2017;34:104–14. https://doi.org/10.1016/j.rbmo.2016.10.005.
14. Qin X, Zhao Y, Zhang T, Yin C, Qiao J, Guo W, Lu B. TrkB agonist antibody ameliorates fertility deficits in aged and cyclophosphamide-induced premature ovarian failure model mice. Nat Commun. 2022. https://doi.org/10.1038/s41467-022-28611-2.
15. Eppig JJ, Reproduction. Oocytes call, granulosa cells connect. Curr Biol. 2018;28:R354–6. https://doi.org/10.1016/j.cub.2018.03.005.
16. Zhang Y, Yan Z, Qin Q, Nisenblat V, Chang H-M, Yu Y, et al. Transcriptome landscape of human folliculogenesis reveals oocyte and granulosa cell interactions. Mol Cell. 2018;72:1021–e10344. https://doi.org/10.1016/j.molcel.2018.10.029.
17. Diaz FJ, Wigglesworth K, Eppig JJ. Oocytes determine cumulus cell lineage in mouse ovarian follicles. J Cell Sci. 2007;120:1330–40. https://doi.org/10.1242/jcs.000968.
18. Eppig JJ. Oocyte control of ovarian follicular development and function in mammals. Reproduction. 2001;122:829–38. https://doi.org/10.1530/rep.0.1220829.
19. Edson MA, Nagaraja AK, Matzuk MM. The mammalian ovary from genesis to revelation. Endocr Rev. 2009;30:624–712. https://doi.org/10.1210/er.2009-0012.
20. Fan Y, Chang Y, Wei L, Chen J, Li J, Goldsmith S, et al. Apoptosis of mural granulosa cells is increased in women with diminished ovarian reserve. J Assist Reprod Genet. 2019;36:1225–35. https://doi.org/10.1007/s10815-019-01446-5.
21. Yuksel A, Bildik G, Senbabaoglu F, Akin N, Arvas M, Unal F, et al. The magnitude of gonadotoxicity of chemotherapy drugs on ovarian follicles and granulosa cells varies depending upon the category of the drugs and the type of granulosa cells. Hum Reprod. 2015;30:2926–35. https://doi.org/10.1093/humrep/dev256.
22. Sugiura K, Su Y-Q, Diaz FJ, Pangas SA, Sharma S, Wigglesworth K, et al. Oocyte-derived BMP15 and FGFs cooperate to promote Glycolysis in cumulus cells. Development. 2008;135:786. https://doi.org/10.1242/dev.020024.
23. Gao E-M, Turathum B, Wang L, Di Zhang, Liu Y-B, Tang R-X, Chian R-C. The differential metabolomes in cumulus and mural granulosa cells from human preovulatory follicles. Reprod Sci. 2022;29:1343–56. https://doi.org/10.1007/s43032-021-00691-3.
24. Du Y, Carranza Z, Luan Y, Busman-Sahay K, Wolf S, Campbell SP, et al. Evidence of cancer therapy-induced chronic inflammation in the ovary across multiple species: A potential cause of persistent tissue damage and follicle depletion. J Reprod Immunol. 2022;150:103491. https://doi.org/10.1016/j.jri.2022.103491.
25. Luan Y, Edmonds ME, Woodruff TK, Kim S-Y. Inhibitors of apoptosis protect the ovarian reserve from cyclophosphamide. J Endocrinol. 2019;240:243–56. https://doi.org/10.1530/JOE-18-0370.
26. Stringer J, Groenewegen E, Liew SH, Hutt K. NMN does not protect the ovarian reserve from cancer treatments. Reproduction. 2020;159:105–13. https://doi.org/10.1530/REP-19-0337.
27. Sugiura K, Pendola FL, Eppig JJ. Oocyte control of metabolic cooperativity between oocytes and companion granulosa cells: energy metabolism. Dev Biol. 2005;279:20–30. https://doi.org/10.1016/j.ydbio.2004.11.027.
28. Zhang M, Su Y-Q, Sugiura K, Wigglesworth K, Xia G, Eppig JJ. Estradiol promotes and maintains cumulus cell expression of natriuretic peptide receptor 2 (NPR2) and meiotic arrest in mouse oocytes in vitro. Endocrinology. 2011;152:4377–85. https://doi.org/10.1210/en.2011-1118.
29. Yoo M, Tanaka T, Konishi H, Tanabe A, Taniguchi K, Komura K, et al. The protective effect of testosterone on the ovarian reserve during cyclophosphamide treatment. Onco Targets Ther. 2020;13:2987–95. https://doi.org/10.2147/OTT.S242703.
30. Bellusci G, Mattiello L, Iannizzotto V, Ciccone S, Maiani E, Villani V, et al. Kinase-independent Inhibition of cyclophosphamide-induced pathways protects the ovarian reserve and prolongs fertility. Cell Death Dis. 2019;10:726. https://doi.org/10.1038/s41419-019-1961-y.
31. Yang W, Ma Y, Jin J, Ren P, Zhou H, Xu S, et al. Cyclophosphamide exposure causes Long-Term detrimental effect of oocytes developmental competence through affecting the epigenetic modification and maternal factors' transcription during oocyte growth. Front Cell Dev Biol. 2021;9:682060. https://doi.org/10.3389/fcell.2021.682060.
32. Richani D, Sutton-McDowall ML, Frank LA, Gilchrist RB, Thompson JG. Effect of epidermal growth factor-like peptides on the metabolism of in vitro-matured mouse oocytes and cumulus cells. Biol Reprod. 2014;90:49. https://doi.org/10.1095/biolreprod.113.115311.
33. Xie X, Hu H, Tong X, Li L, Liu X, Chen M, et al. The mTOR-S6K pathway links growth signalling to DNA damage response by targeting RNF168. Nat Cell Biol. 2018;20:320–31. https://doi.org/10.1038/s41556-017-0033-8.
34. Sadat Tahajjodi S, Farashahi Yazd E, Agha-Rahimi A, Aflatoonian R, Ali Khalili M, Mohammadi M, Aflatoonian B. Biological and physiological characteristics of human cumulus cells in adherent culture condition. Int J Reprod Biomed. 2019;18:1–10. https://doi.org/10.18502/ijrm.v18i1.6189.
35. Su Y-Q, Sugiura K, Eppig JJ. Mouse oocyte control of granulosa cell development and function: paracrine regulation of cumulus cell metabolism. Semin Reprod Med. 2009;27:32–42. https://doi.org/10.1055/s-0028-1108008.
36. Yamochi T, Hashimoto S, Morimoto Y. Mural granulosa cells support to maintain the viability of growing Porcine oocytes and its developmental competence after insemination. J Assist Reprod Genet. 2021;38:2591–9. https://doi.org/10.1007/s10815-021-02212-2.
37. Madogwe E, Tanwar DK, Taibi M, Schuermann Y, St-Yves A, Duggavathi R. Global analysis of FSH-regulated gene expression and histone modification in mouse granulosa cells. Mol Reprod Dev. 2020;87:1082–96. https://doi.org/10.1002/mrd.23419.
38. Devos M, Grosbois J, Demeestere I. Interaction between PI3K/AKT and Hippo pathways during in vitro follicular activation and response to fragmentation and chemotherapy exposure using a mouse immature ovary model. Biol Reprod. 2020;102:717–29. https://doi.org/10.1093/biolre/ioz215.
39. Wigglesworth K, Lee K-B, Emori C, Sugiura K, Eppig JJ. Transcriptomic diversification of developing cumulus and mural granulosa cells in mouse ovarian follicles. Biol Reprod. 2015;92:23. https://doi.org/10.1095/biolreprod.114.121756.

40. Kaufmann WK, Paules RS. DNA damage and cell cycle checkpoints. FASEB J. 1996;10:238–47. https://doi.org/10.1096/fasebj.10.2.8641557.
41. Ma Y, Vassetzky Y, Dokudovskaya S. mTORC1 pathway in DNA damage response. Biochim Biophys Acta Mol Cell Res. 2018;1865:1293–311. https://doi.org/10.1016/j.bbamcr.2018.06.011.
42. Shen C, Oswald D, Phelps D, Cam H, Pelloski CE, Pang Q, Houghton PJ. Regulation of FANCD2 by the mTOR pathway contributes to the resistance of cancer cells to DNA double-strand breaks. Cancer Res. 2013;73:3393–401. https://doi.org/10.1158/0008-5472.CAN-12-4282.

Publisher's note